

BULLETIN
DE
L'ACADÉMIE POLONAISE
DES SCIENCES

Rédacteur en chef
K. KURATOWSKI

Rédacteur en chef suppléant
S. KULCZYŃSKI

CLASSE TROISIÈME

Rédacteur de la Série
L. INFELD

Comité de Rédaction de la Série
K. BORSUK, S. LESZCZYCKI, J. SAMSONOWICZ, M. ŚMIAŁOWSKI

VOLUME II
NUMÉRO 8

VARSOVIE 1954

PRINTED IN POLAND

PAŃSTWOWE WYDAWNICTWO NAUKOWE — WARSZAWA 1954

<i>Nakład 1036 + 100 egz.</i>	<i>Rękopis dostarczono 26. VII. 1954</i>
<i>Ark. wyd. 3⁵, druk, 3+1 tabl.</i>	<i>Podpisano do druku 10. XI. 1954</i>
<i>Papier bezdrzewny sat. 80 g kl. III</i>	<i>Druk ukończono 20. XI. 1954</i>
<i>Format B5, 70×100 cm</i>	<i>Zam. prod. 417/54 Cena zł 5,—</i>

KRAKOWSKA Drukarnia naukowa, KRAKÓW, UL. CZAPSKICH 4

On Abelian Groups - Every Countable Subgroup of which is an Endomorphic Image

by

E. SĄSIADA

Presented by K. KURATOWSKI on June 2, 1954

1. Problems. In their paper [1] A. Kertesz and T. Szele proposed the following problem:

Determine the structure of groups G possessing the property:

(P) *every subgroup of G is an endomorphic image of G .*

According to the authors themselves, the problem seems difficult even in the case of abelian groups. In one of their later papers [2] A. Kertesz and T. Szele made the first step towards the solution of this problem for abelian groups. They determined the structure of abelian groups G possessing the property:

(I) *Every finitely generated subgroup of G is an endomorphic image of G , which is weaker than (P).*

In the present paper we shall investigate the structure of abelian groups G possessing the property:

(II) *Every countable subgroup of G is an endomorphic image of G .*

Property (II) is in fact stronger than property (I), but it is at the same time weaker than property (P).

Thus the determination of the structure of abelian groups possessing property (II) is a further step towards the solution of the above-mentioned problem for abelian groups. It also gives the solution of this problem in the case of countable abelian groups.

The two following theorems present the solution of the problem of determining all abelian groups which have property (II).

Theorem 1. *In order for a torsion abelian group T to possess property (II) it is necessary and sufficient that:*

(*) *every primary component T_p of T be either a bounded group (i. e. the orders of elements in T_p are bounded in common), or an abelian exten-*

sion of a certain p -group N_p with the group $F_p = \sum_{n=1}^{\infty} C(p^n)$ (i. e. the factor group T_p/N_p is isomorphic to F_p).

Theorem 2. *In order for an abelian group G to possess property (II) it is necessary and sufficient that either group G contain a direct summand, which is a direct sum of an infinite number of infinite cyclic groups, or that G have the form $G = H + U$, where U is a direct sum of a finite number of infinite cyclic groups (or $U = \{0\}$), and H is a torsion group possessing property (*).*

2. Lemma 1. *An abelian group decomposable into a direct sum of cyclic groups has property (P).*

This lemma is the consequence of the well known fact, that every subgroup of a group which is decomposable into a direct sum of cyclic groups is also decomposable into a direct sum of cyclic groups (see Kulikoff [3]).

Lemma 2. *In order for a torsion abelian group T to possess property (II) it is necessary and sufficient that every primary component T_p possess property (II).*

This lemma is evident. It is also true for property (P).

The following lemma is evident too:

Lemma 3. *Every countable abelian p -group is a homomorphic image of the group $F_p = \sum_{n=1}^{\infty} C(p^n)$.*

3. Proof of theorem 1. Let T_p be a primary component of the torsion abelian group T possessing property (II). By lemma 2 group T_p possesses property (II). Let us assume that group T_p is not bounded. We shall see that in this case group T_p contains a subgroup isomorphic to F_p , which is enough to prove the necessity of condition (*).

Let B_p be a basic subgroup of the group T_p , i. e.

1° B_p is a serving subgroup of T_p ,

2° B_p is a direct sum of cyclic groups,

3° the factor group T_p/B_p is an algebraically closed group. The existence of such a subgroup is proved by Kulikoff [3].

The group B_p cannot be bounded. In fact, according to the well known theorem of Prüfer (see [4]), if group B_p were bounded, then in view of 1° group B_p would be a direct summand of group T_p , and therefore $T_p = B_p + D_p$, where D_p is an algebraically closed group.

On the other hand, as group T_p is not bounded, there is in T_p an element g , the order of which is greater than the order of every element of group B_p , and, as group T_p possesses property (II), there exists an endomorphism ε , such that $\varepsilon(T_p) = \{g\}$. Evidently $\varepsilon(D_p) = \{0\}$ and therefore $\varepsilon(B_p) = \{g\}$ which is impossible as the orders of the elements of group B_p are smaller than the order of the element g .

Thus it follows that the basic subgroup B_p , and more obviously group T_p , contains a subgroup isomorphic to the group F_p .

Now let every primary component T_p of the torsion abelian group T be either: a) a bounded group, or b) an abelian extension of a certain p -group N_p with group F_p . In case a) T_p is decomposable into a direct sum of cyclic groups [4], and by lemma 1 group T_p has property (II). In case b) the factor group T_p/N_p is isomorphic to group F_p and by virtue of lemma 3 group T_p also has property (II).

It follows from lemma 2 that group T has property (II) as well.

4. Proof of theorem 2. Let G be an abelian group possessing property (II). Let us examine the rank of group G , i. e. the power of the maximal system of independent elements in G . If the rank is infinite, then evidently group G contains a subgroup V which is a direct sum of an infinite number of infinite cyclic groups and, since group G has property (II), its endomorphic image. It follows that group G contains a direct summand which is isomorphic to group V .

If the rank of group G is finite, then group G may be represented as a direct sum $G = H + U$, where U is a direct sum of a finite number of infinite cyclic groups (or $U = \{0\}$), and H is a torsion group. It is easy to see that H must have property (II). In fact, let H_0 be a countable subgroup H and η an endomorphism of G onto the subgroup $G_0 = H_0 + U$ (the existence of which is assumed). It is evident that $\eta(H) = H_0$.

From theorem 1 it follows that group H has property (*).

Conversely: if an abelian group G contains a direct summand which is a direct sum of an infinite number of infinite cyclic groups, then evidently group G has property (II). If group G has the form $G = H + U$, where H is a torsion group possessing property (*), and U is a direct sum of a finite number of infinite cyclic groups, then each of its countable subgroups G_1 may be represented in the form:

(1) $G_1 = H_1 + U_1$, where $H_1 \subset H$, and U_1 is a direct sum of infinite cyclic groups.

In fact: let H_1 be a torsion subgroup in G_1 . Evidently $H_1 = G_1 \cap H$. From the first theorem on isomorphism it follows that $\{G_1, H\}/H \cong G_1/H_1$. As $\{G_1, H\}/H \subset G/H \cong U$, the factor group G_1/H_1 is isomorphic to the subgroup of group U , and therefore it is a direct sum of infinite cyclic groups and on this account G_1 may be represented in form (1).

From the assumption that H has property (*) and from theorem 1 it follows that there exists an endomorphism ε_1 such that $\varepsilon_1(H) = H_1$. On the other hand there exists a homomorphism ε_2 such that $\varepsilon_2(U) = U_1$. Evidently $\varepsilon = \varepsilon_1 + \varepsilon_2$ is an endomorphism of G onto G_1 .

5. Remarks. Theorem 1 and theorem 2 yield:

Theorem 3. *In order for a countable abelian group G to have property (P) it is necessary and sufficient that either group G contain a direct summand which is a direct sum of an infinite number of infinite cyclic groups, or it have the form $G = H + U$, where U is a direct sum of a finite number of infinite cyclic groups (or $U = \{0\}$) and is a torsion group possessing property (*).*

Theorem 3 gives the solution of A. Kertesz's and T. Szele's problem in the case of countable abelian groups. This problem can also be easily solved for torsion-free abelian groups; namely, as is known, the rank of a torsion-free abelian group, if it is not finite, is equal to the power of the same group; therefore we have:

Theorem 4. *In order for a torsion-free abelian group G to have property (P) it is necessary and sufficient that it be either finitely generated or can be represented in the form $G = H + U$, where $U = \sum_{g \in G} C_{\infty}^{(g)}$ (by $C_{\infty}^{(g)}$ we denote the infinite cyclic group corresponding to the element $g \in G$).*

Institute of Mathematics, Polish Academy of Sciences

REFERENCES

- [1] Kertesz A., Szele T., *On Abelian Groups Every Multiple of which is a Direct Summand*, Acta Sc. Math. **14** (1952).
- [2] Kertesz A., Szele T., *Abelian Groups Every Finitely Generated Subgroup of which is an Endomorphic Image*, Acta Sc. Math. **15** (1953), 70.
- [3] Kulikoff L. J., *K teorii abielewycy grupp proizwolnoj moszcznosti*, Mat. Sbornik **16** (1945).
- [4] Prüfer H., *Untersuchungen über die Zerlegbarkeit der abzählbaren primären abelschen Gruppen*, Math. Zeitschr. (1923), 35.

Probabilité de la sécurité d'une construction mécanique

par

W. POGORZELSKI

Présenté par H. STEINHAUS à la séance du 24 Avril 1954

Ce travail est une continuation du travail publié sous le même titre en langue polonaise [1].

Soit une construction mécanique composée de n parties liées, U_1, U_2, \dots, U_n , obéissant aux lois de la théorie de l'élasticité. Dans le travail cité nous avons calculé la probabilité de la sécurité de cette construction en admettant, à cause des inexactitudes accidentelles de la production, que les paramètres qui déterminent la forme géométrique et les propriétés physiques de la construction sont des variables aléatoires obéissant à une des lois de probabilité, par exemple à celle de Gauss.

Mais, en réalité, non seulement les paramètres mentionnés éprouvent des écarts accidentels, mais la forme même des surfaces (planes ou sphériques) des parties de la construction éprouve des écarts accidentels à cause de l'inexactitude de la production industrielle. De même les lois physiques (par exemple la loi de Hooke) qui lient les tensions avec les déformations ne sont pas certaines mais éprouvent des écarts fonctionnels aléatoires.

Supposons que notre construction soit soumise à l'action des forces extérieures données. Désignons par $\sigma_1, \sigma_2, \dots, \sigma_n$ les bornes supérieures des modules des tensions dans chaque partie U_1, U_2, \dots, U_n , que l'on calculera en résolvant un problème aux limites des équations différentielles de la théorie de l'élasticité. D'après nos remarques, ces tensions seront les résultats de certaines opérations fonctionnelles

$$(1) \quad \sigma_v = \hat{O}_v[f_1, f_2, \dots, f_\alpha] \quad (v = 1, 2, \dots, n),$$

où $f_1, f_2, \dots, f_\alpha$ désignent les fonctions qui déterminent les surfaces de la construction, les liaisons et qu'on peut appeler *fonctions aléatoires*. Les conditions de la sécurité de la construction s'expriment par les inégalités

$$2) \quad \sigma_1 < R_1; \sigma_2 < R_2; \dots; \sigma_n < R_n,$$

où R_1, R_2, \dots, R_n désignent les valeurs limites des tensions dépendant des

matériaux de la construction et déterminées par l'expérience. Pour calculer effectivement la probabilité de la sécurité, nous supposons que les fonctions aléatoires forment des familles de fonctions des variables u_1, u_2, \dots, u_p

$$(3) \quad f_\nu = F_\nu(u_1, u_2, \dots, u_p, q_1, q_2, \dots, q_m) \quad (\nu = 1, 2, \dots, \alpha)$$

et des paramètres aléatoires, q_1, q_2, \dots, q_m , dont les écarts accidentels obéissent à une des lois de probabilité, par exemple à celle de Gauss:

$$(4) \quad \frac{1}{s_\nu \sqrt{2\pi}} \exp \left[-\frac{(q_\nu - q_\nu^{(0)})^2}{2s_\nu^2} \right] \quad (\nu = 1, 2, \dots, m),$$

$q_\nu^{(0)}$ étant les espérances mathématiques de q_ν , s_ν — les écarts moyens. L'augmentation du nombre des paramètres aléatoires q_1, q_2, \dots, q_m , élève l'exactitude du raisonnement, puisqu'elle approche les fonctions choisies (3) vers la réalité. L'hypothèse (3) étant admise, on obtient, tout calcul fait, les tensions $\sigma_1, \sigma_2, \dots, \sigma_n$ sous la forme des fonctions

$$(5) \quad \sigma_\nu = \Phi_\nu(q_1, q_2, \dots, q_m) \quad (\nu = 1, 2, \dots, n)$$

des paramètres q_1, q_2, \dots, q_m , déterminées dans un domaine D d'espace des points aux coordonnées rectangulaires, q_1, q_2, \dots, q_m .

La sécurité de la construction s'exprime alors par les inégalités

$$(6) \quad \Phi_\nu(q_1, q_2, \dots, q_m) < R_\nu \quad (\nu = 1, 2, \dots, n),$$

qui définissent un domaine $\Lambda(R_1, R_2, \dots, R_n)$ dans l'espace des points q_1, q_2, \dots, q_m . Les bornes positives R_1, R_2, \dots, R_n étant fixées, la probabilité pour que le point (q_1, q_2, \dots, q_m) soit situé dans le domaine (6) s'exprime, sous la supposition (3), par l'intégrale

$$(7) \quad P(R_1, R_2, \dots, R_n) = \int \int \dots \int_{\Lambda} \frac{1}{s_1 s_2 \dots s_m (\sqrt{2\pi})^m} \exp \left[-\sum_{\nu=1}^m \frac{(q_\nu - q_\nu^{(0)})^2}{2s_\nu^2} \right] dq_1 \dots dq_m.$$

Cette intégrale est une fonction des paramètres R_1, R_2, \dots, R_n , définie dans un domaine à n dimensions Λ dépendant des inégalités (6).

Les paramètres R_1, R_2, \dots, R_n sont aussi des variables aléatoires pour lesquelles nous admettons la loi normale de probabilités

$$(8) \quad \frac{1}{s'_\nu \sqrt{2\pi}} \exp \left[-\frac{(R_\nu - R_\nu^{(0)})^2}{2s'^2_\nu} \right] \quad (\nu = 1, 2, \dots, n).$$

Nous en concluons que la probabilité absolue de la sécurité de la construction mécanique s'exprime par l'intégrale

$$(9) \quad \Pi_{abs} = \int \int \dots \int_{\Delta} \frac{P(R_1, R_2, \dots, R_n)}{s'_1 s'_2 \dots s'_n (\sqrt{2\pi})^n} \exp \left[-\sum_{\nu=1}^n \frac{(R_\nu - R_\nu^{(0)})^2}{2s'^2_\nu} \right] dR_1 \dots dR_n.$$

Nos considérations concernaient la probabilité de la sécurité dans un instant initial déterminé. Mais la forme même de la construction et l'état physique des matériaux change avec le temps par l'usage. Cherchons donc la probabilité de la sécurité aux moments futurs. Dans ce but supposons que les espérances $q_v^{(0)}$, $R_v^{(0)}$ varient avec le temps suivant les lois empiriques de la forme

$$(10) \quad \begin{aligned} q_v^{(0)}(t) &= q_v^{(0)}(0) + \sum_{\alpha=1}^{\lambda_v} A_{v\alpha} \varphi_{v\alpha}(t), \\ R_v^{(0)}(t) &= R_v^{(0)}(0) + \sum_{\alpha=1}^{\lambda'_v} B_{v\alpha} \psi_{v\alpha}(t), \end{aligned}$$

où toutes les fonctions $\varphi_{v\alpha}$ et $\psi_{v\alpha}$ s'annulent au moment initial $t=0$. Si la loi de variation avec le temps (10) est sûre, la substitution des expressions (10) dans les intégrales (7) et (9) permet de calculer la probabilité de la sécurité au moment futur t arbitraire. Mais en réalité les lois de variation (10) ne sont que probables et les paramètres $A_{v\alpha}$, $B_{v\alpha}$ sont des variables aléatoires avec les répartitions des probabilités

$$(11) \quad \frac{1}{s''_{v\alpha} \sqrt{2\pi}} \exp \left[-\frac{(A_{v\alpha} - A_{v\alpha}^{(0)})^2}{2 s''_{v\alpha}{}^2} \right], \quad \frac{1}{s'''_{v\alpha} \sqrt{2\pi}} \exp \left[-\frac{(B_{v\alpha} - B_{v\alpha}^{(0)})^2}{2 s'''_{v\alpha}{}^2} \right].$$

En multipliant les expressions (7) et (9) par tous les facteurs (11) et en intégrant pour toutes les valeurs des variables $A_{v\alpha}$, $B_{v\alpha}$, on obtient la probabilité cherchée aux moments futurs t .

Le calcul se simplifie grâce à la propriété connue de la distribution de Gauss concernant la fonction linéaire des variables aléatoires. Notamment, pour obtenir la probabilité cherchée, il suffit de faire un calcul identique aux précédents (7) et (9), en remplaçant dans la fonction (4) l'écart moyen s_v par

$$\sqrt{\sum_{\alpha=1}^{\lambda_v} \varphi_{v\alpha}^2(t) \cdot s''_{v\alpha}{}^2}$$

et la valeur moyenne $q_v^{(0)}$ par l'expression

$$q_v^{(0)}(0) + \sum_{\alpha=1}^{\lambda_v} A_{v\alpha} \varphi_{v\alpha}(t).$$

On calculera ensuite la probabilité de la sécurité au moment futur t , en remplaçant sous le signe de l'intégrale (9) l'écart moyen s'_v par l'expression

$$\sqrt{\sum_{\alpha=1}^{\lambda'_v} \psi_{v\alpha}^2(t) s'''_{v\alpha}{}^2}$$

et la valeur moyenne $R_{v\alpha}^{(0)}$ par la somme

$$R_v^{(0)}(0) + \sum_{\alpha=1}^{\lambda'_v} B_{v\alpha}^{(0)} \psi_{v\alpha}(t).$$

Institut Mathématique de l'Académie Polonaise des Sciences

OUVRAGES CITÉS

[1] Pogorzelski W., *Prawdopodobieństwo bezpieczeństwa konstrukcji*, Zastosowania Matematyki 2, No 1 (1954).

Problème aux limites d'Hilbert généralisé

par

W. POGORZELSKI

Présenté par S. MAZUR le 28 Juin 1954

Soit, dans le plan de la variable complexe, un ensemble de p lignes de Jordan L_1, L_2, \dots, L_p disjointes et délimitant respectivement les domaines disjoints S_1, S_2, \dots, S_p . Soit en outre L_0 une ligne de Jordan embrassant toutes les lignes précédentes. Désignons par S_0^- le domaine infini situé à l'extérieur de la ligne L_0 et par S^+ le domaine limité par la ligne L_0 et les lignes L_1, L_2, \dots, L_p . Dans les travaux [1] et [2], le problème suivant a été posé: *trouver le système de fonctions de la variable complexe $\Phi_1(z), \dots, \Phi_m(z)$ dont chacune soit holomorphe dans les domaines $S^+, S_0^-, S_1^-, \dots, S_p^-$ séparément et dont les valeurs limites $\Phi_\alpha^+(t)$ et $\Phi_\alpha^-(t)$ satisfassent en tout point t de l'ensemble $L = L_0 + L_1 + \dots + L_p$ aux m relations*

$$(1) \quad \Phi_\alpha^+(t) = G_\alpha(t) \Phi_\alpha^-(t) + \lambda F_\alpha[t, \Phi_1^+(t), \dots, \Phi_m^+(t), \Phi_1^-(t), \dots, \Phi_m^-(t)],$$

où $\alpha = 1, 2, \dots, m$, les fonctions $G_\alpha(t)$ sont définies sur les lignes L_0, L_1, \dots, L_p et $F_\alpha(t, u_1, u_2, \dots, u_{2m})$ sont des fonctions données de $2m + 1$ arguments.

Dans les deux travaux précités ce problème a été résolu sous l'hypothèse que les fonctions G_α et F_α sont holomorphes dans certaines bandes comprenant les lignes L . Dans le travail présent, le problème (1) sera résolu sous les hypothèses plus générales suivantes:

I. Les fonctions $G_\alpha(t)$ sont définies sur les lignes L , elles y sont différentes de zéro et satisfont à la condition d'Hölder

$$|G_\alpha(t') - G_\alpha(t)| < k|t' - t|^\mu.$$

II. Les fonctions $F_\alpha(t, u_1, u_2, \dots, u_{2m})$ sont définies dans le domaine

$$(2) \quad t \in L, \quad |u_\nu| \leq R \quad (\nu = 1, 2, \dots, 2m)$$

et elles y vérifient la condition d'Hölder par rapport à la variable t , ainsi que la condition de Lipschitz par rapport aux variables u_1, u_2, \dots, u_{2m} .

III. Les lignes $L_0, L_1, L_2, \dots, L_p$ ont les tangentes continues en tout point.

D'après les travaux [1] et [2], l'on peut affirmer que sous les hypothèses I, II et III la formule

$$(3) \quad \Phi_{\alpha}(z) = \frac{\lambda}{2\pi i} X_{\alpha}(z) \int_L \frac{F_{\alpha}[\tau, \varphi_1(\tau), \dots, \varphi_{2m}(\tau)]}{X_{\alpha}^{+}(\tau)(\tau - z)} d\tau + X_{\alpha}(y) P_{\alpha}(z),$$

où $\alpha = 1, 2, \dots, m$, donne la solution du problème ainsi généralisé, si les $2m$ fonctions $\varphi_1(\tau), \dots, \varphi_{2m}(\tau)$ satisfont à la condition d'Hölder et au système d'équations intégrales singulières (intégrales au sens de Cauchy), en tout point $t \in L$

$$(4) \quad \varphi_{\alpha}(t) = \lambda F_{\alpha}^{*}[t, \varphi_1(t), \dots, \varphi_{2m}(t)] + \lambda \int_L \frac{F_{\alpha}^{**}[t, \tau, \varphi_1(\tau), \dots, \varphi_{2m}(\tau)]}{\tau - t} d\tau + f_{\alpha}(t),$$

où $\alpha = 1, 2, \dots, 2m$. Dans les formules (3) et (4) $X_{\alpha}(z)$ est la solution dite canonique du problème homogène d'Hilbert (c'est-à-dire satisfaisant à la condition limite $X_{\alpha}^{+}(t) = G_{\alpha}(t) X_{\alpha}^{-}(t)$ et ayant le plus petit ordre à l'infini), $P_{\alpha}(z)$ est une fonction entière arbitraire et les fonctions

$$(5) \quad F_{\alpha}^{*}(t, u_1, u_2, \dots, u_{2m}), F_{\alpha}^{**}(t, \tau, u_1, u_2, \dots, u_{2m}), f_{\alpha}(t)$$

sont définies dans le domaine (2) par de simples opérations rationnelles sur les fonctions F_{α} , X_{α} et P_{α} considérées dans le travail [2].

On est donc amené à résoudre le système d'équations intégrales (4). D'après les hypothèses I et II, il existe une constante $\mu < 1$ telle que les fonctions (5) satisfont dans le domaine (2) aux trois inégalités

$$(6) \quad \begin{aligned} |F_{\alpha}^{*}(t, u_1, \dots, u_{2m}) - F_{\alpha}^{*}(t', u'_1, \dots, u'_{2m})| &< A[|t - t'|^{\mu} + \sum_{\nu=1}^{2m} |u_{\nu} - u'_{\nu}|], \\ |F_{\alpha}^{**}(t, \tau, u_1, \dots, u_{2m}) - F_{\alpha}^{**}(t', \tau', u'_1, \dots, u'_{2m})| &< \\ &< B[|t - t'|^{\mu} + |\tau - \tau'|^{\mu} + \sum_{\nu=1}^{2m} |u_{\nu} - u'_{\nu}|], \\ |f_{\alpha}(t) - f_{\alpha}(t')| &< C|t - t'|^{\mu}, \end{aligned}$$

A, B et C étant des constantes positives. Cependant les inégalités (6) ne suffisent pas pour résoudre le système (4) par la méthode des approximations successives. C'est pourquoi il va être résolu par l'application du théorème suivant de Schauder [3] sur le point invariant (basé sur les propriétés topologiques des espaces métriques): "Toute transformation continue d'un ensemble convexe, borné, fermé et contenu dans un espace linéaire, normé et complet, en un sous-ensemble compact a au moins un point invariant". Le raisonnement aura recours en outre à la propriété importante de l'intégrale du type de Cauchy

$$(7) \quad \psi(t) = \int_L \frac{\varphi(\tau) d\tau}{\tau - t}$$

démontrée par Plemelj [4] et ensuite, plus rigoureusement, par Privaloff [5] (cf. aussi [6]): si la fonction $\varphi(t)$ satisfait à la condition d'Hölder en tout point $t \in L$, il en est de même de la fonction $\psi(t)$. De plus, lorsque l'exposant μ d'Hölder est inférieur à 1 et que

$$(8) \quad |\varphi(t) - \varphi(t')| < D|t - t'|^\mu,$$

la même valeur de $\mu < 1$ est valable pour la fonction ψ et

$$(9) \quad |\psi(t) - \psi(t')| < KD|t - t'|^\mu,$$

où le coefficient K ne dépend que de la forme géométrique des lignes L .

Considérons maintenant l'espace fonctionnel E composé de tous les systèmes de $2m$ fonctions continues complexes $U[\varphi_1(t), \dots, \varphi_{2m}(t)]$ définies en tout point $t \in L^*$. On définit la distance $\delta(U, V)$ entre deux points $U[\varphi_1(t), \dots, \varphi_{2m}(t)]$ et $V[g_1(t), \dots, g_{2m}(t)]$ de l'espace E par la somme des bornes supérieures

$$(10) \quad \delta(U, V) = \sum_{\alpha=1}^{2m} \sup |\varphi_\alpha(t) - g_\alpha(t)|.$$

Ensuite, on définit le produit d'un point U par un nombre réel γ et la somme de deux points U et V par les formules

$$\gamma \cdot U = [\gamma \varphi_1, \gamma \varphi_2, \dots, \gamma \varphi_{2m}] \quad \text{et} \quad U + V = [\varphi_1 + g_1, \varphi_2 + g_2, \dots, \varphi_{2m} + g_{2m}]$$

respectivement. Grâce à certaines hypothèses supplémentaires, l'espace E est métrique, complet, normé et linéaire.

Soit $S(\kappa, \mu)$ l'ensemble de tous les points $U(\varphi_1, \dots, \varphi_{2m})$ de l'espace E qui satisfont à la condition

$$(11) \quad |\varphi_\alpha| \leq R \quad (\alpha = 1, 2, \dots, 2m)$$

et à celle d'Hölder

$$(12) \quad |\varphi_\alpha(t) - \varphi_\alpha(t')| \leq \kappa |t - t'|^\mu \quad (\alpha = 1, 2, \dots, 2m)$$

où κ est une constante positive fixée arbitrairement et $\mu < 1$ est l'exposant d'Hölder qui figure dans les inégalités (6). Il est facile de montrer que l'ensemble $S(\kappa, \mu)$ est fermé et convexe.

En tenant compte de la forme des équations intégrales (4), appliquons aux points de l'ensemble S la transformation fonctionnelle définie par les relations

$$(13) \quad \psi_\alpha(t) = \lambda F_\alpha^*[t, \varphi_1(t), \dots, \varphi_{2m}(t)] + \lambda \int_L \frac{F_\alpha^{**}[t, \tau, \varphi_1(\tau), \dots, \varphi_{2m}(\tau)]}{\tau - t} d\tau + f_\alpha(t).$$

On montre, en s'appuyant sur les inégalités (6) et sur la propriété (9) de l'intégrale (7), que le transformé S' de S est contenu dans S , pourvu

*) Je dois à S. Mazur la suggestion d'employer ici l'espace des fonctions continues au lieu de celui des fonctions assujetties à la condition d'Hölder.

que les modules du paramètre λ et des fonctions $P_\alpha(t)$ soient suffisamment petits. Puis, en s'appuyant sur le théorème d'Arzelà concernant les familles de fonctions continues, on montre que le transformé S' est compact. On montre enfin que la transformation fonctionnelle (13) est continue. Il en résulte, d'après le théorème précité de Schauder, l'existence d'un point invariant de la transformation (13) et, par conséquent, l'existence de la solution du système d'équations intégrales (4), qui fournit la solution (3) du problème généralisé d'Hilbert.

Un exposé plus détaillé sera publié sous le même titre dans les "Annales Polonici Mathematici".

Institut Mathématique de l'Académie Polonaise des Sciences

OUVRAGES CITÉS

- [1] Pogorzelski W., *Problème non linéaire d'Hilbert pour le système de fonctions*, Bull. Acad. Polon. Sci., Cl. III, **2** (1954), 5.
- [2] — *Annales Polonici Mathematici*, **2** (1954).
- [3] Schauder J., *Der Fixpunktsatz in Funktionalräumen*, Studia Mathematica, **2** (1930).
- [4] Plemelj J., *Ein Ergänzungssatz zur Cauchyschen Integraldarstellung*, Monatshefte für Mathem. u. Physik 1908, 205.
- [5] Privaloff I. I., *Granitchnyé svoïstva analititcheskikh funktsii*, Izdat. Moskovskogo Universiteta, 1941.
- [6] Mouschelichvili N. I., *Singularnyie intiegralnyie uravniénia*, Moscou, 1945, 47.

Limit Properties of Homogeneous Markoff Processes with a Denumerable Set of States

by

K. URBANIK

Presented by H. STEINHAUS on June 12, 1954

1. A homogeneous stochastic Markoff process with a denumerable set of possible states E_0, E_1, E_2, \dots is usually described by defining the transition probability $P_k^n(t)$, i. e. the conditional probability of the transition from the state E_k to the state E_n in time t .

Let Ω be a set of non-negative integral-valued functions $\omega(t)$ defined for $t \geq 0$ and such that $\omega(0) = \alpha$ (where α is arbitrary, but fixed).

Let us denote by B_Ω the σ -field of sets spanned by all the sets of the form

$$A(t, n) = \{\omega \in \Omega : \omega(t) = n\}.$$

The transition probabilities $P_k^n(t)$ determine a probability measure Pr in the field B_Ω , which for $0 = t_0 \leq t_1 \leq \dots \leq t_n$ and for any k_1, k_2, \dots, k_n satisfies the condition

$$Pr \prod_{j=1}^n \left\{ \omega : \omega(t_j) = k_j \right\} = \prod_{j=1}^n P_{k_{j-1}}^{k_j}(t_j - t_{j-1}),$$

where $k_0 = \alpha$ (see Doob [1], p. 49).

Using the well-known measure-theoretical treatment of stochastic processes, we understand by a *homogeneous Markoff process with denumerably many possible states*, or briefly by a *Markoff process*, the system $\langle \Omega, B_\Omega, Pr \rangle$ defined above.

A Markoff process is called *regular*, if almost all $\omega \in \Omega$ have unilateral limits for every $t \geq 0$. If a Markoff process is regular, then the derivatives

$$a_k^n = \frac{d}{dt} P_k^n(t) \Big|_{t=+0}$$

exist and are called *intensities*. They determine the process (cf. Doob [1], p. 468).

2. Set

$$L(\omega) = \prod_{u \geq 0} \overline{\sum_{t \geq u} \{k: \omega(t) = k\}},$$

where the closure — is considered in the space of all non-negative integers, completed by the limit point ∞ . The set $L(\omega)$ is called the *limit set* of ω . (This notion is proposed by E. Marczewski). It is easy to see that $L(\omega)$ is a one-point set: $L(\omega) = \{l\}$, if and only if there exists a limit in the ordinary sense: $\lim_{t \rightarrow \infty} \omega(t) = l$.

An integer k is called a *limit number* of the process, if

$$\Pr \{ \omega: k \in L(\omega) \} > 0.$$

Theorem 1. *For a regular Markoff process, k is a limit number if and only if*

$$\int_0^{\infty} \Pr \{ \omega: \omega(t) = k \} dt = \infty.$$

A set M of non-negative integers is a *limit set* of the process, if and only if

$$\Pr \{ \omega: L(\omega) = \bar{M} \} > 0.$$

Theorem 1 and some results of P. Lévy ([6], p. 332—346) imply

Theorem 2. *Limit sets of a regular Markoff process are disjoint.*

It is easy to prove that, conversely, every sequence of disjoint sets of non-negative integers forms the system of all limit sets of some regular Markoff process.

It follows from theorems 1 and 2 that, for the birth and death process (i. e. the branching process with a unique kind of particles, cf. [3] and [5]), we have

$$(*) \quad \lim_{t \rightarrow \infty} \omega(t) = 0 \text{ or } \infty$$

with probability 1. This is an answer to a problem raised by H. Steinhaus, in connection with the known fact, that the formula (*) holds in the sense of convergence in probability (see e. g. [3], p. 410).

3. Set $S(\omega) = \sup_{t \geq 0} \omega(t)$. Let F_n denote the conditional distribution function of $S(\omega)$ under the hypothesis $\omega(0) = n$. Using theorem 1 and 2 we can prove

Theorem 3. *For a regular Markoff process the conditional distribution functions F_n satisfy the following system of linear equations:*

$$F_n(k) + \sum_{m \in N_k} F_m(k) A_n^m(k) = B_n(k) \quad \text{for } n \in N_k, \quad k = 0, 1, \dots$$

$$F_n(k) = 0, \quad \text{for } n \text{ non-} \in N_k, \quad k = 0, 1, \dots$$

where

$$A_n^m(k) = \int_0^\infty \left[\sum_{s=k}^\infty a_s^m P_n^s(t) \right] dt$$

$$B_n(k) = \sum_{s \in N_k} \lim_{t \rightarrow \infty} P_n^s(t)$$

$$N_k = \{m : m < k, A_\alpha^m(k) < \infty\}.$$

For the birth and death process with the intensities a_1^0, a_1^1, \dots , we obtain by simple reasoning from theorem 3 and Kolmogoroff's equations ([4], p. 429), the following identity:

$$Pr \left\{ \omega : \max_{t \geq 0} \omega(t) < k \right\} = \begin{cases} 0 & \text{for } k \leq 1 \\ -a_1^0/a_1^1 & \text{for } k = 2 \\ -a_1^0 \Delta_{k-2}/\Delta_{k-1} & \text{for } k \geq 3 \end{cases}$$

where

$$\Delta_k = \begin{vmatrix} a_1^1 a_1^0 & 0 & \dots & 0 & 0 \\ a_1^2 a_1^1 & a_1^0 & \dots & 0 & 0 \\ . & . & . & . & . \\ . & . & . & . & . \\ a_1^k a_1^{k-1} & a_1^{k-2} & \dots & a_1^2 a_1^1 \end{vmatrix},$$

In particular, if $a_1^k = 0$ for $k \geq 3$ (the Feller process; see [3], p. 409), we obtain for $k \geq 1$, setting $a = a_1^0/a_1^2$:

$$Pr \left\{ \omega : \max_{t \geq 0} \omega(t) < k \right\} = \begin{cases} (k-1)/k & \text{if } a = 1 \\ (a - a^k)/(1 - a^k) & \text{if } a \neq 1. \end{cases}$$

The proofs of all theorems given here will be published in *Studia Mathematica*.

Mathematical Institute of Bolesław Bierut University, Wrocław

REFERENCES

- [1] Doob J. L., *Topics in the Theory of Markoff Chains*, Trans. Am. Math. Soc. **52** (1942), 37.
- [2] — *Markoff Chains — Denumerable Case*, Trans. Am. Math. Soc. **58** (1945) 445.
- [3] Feller W., *On the Theory of Stochastic Processes, with Particular Reference to Applications*, Proc. Berkeley Symp. Math. Statistics and Probability 1949, 403—432.
- [4] Kolmogoroff A. N., *Über die analytischen Methoden in der Wahrscheinlichkeitsrechnung*, Math. Annalen **104** (1931), 415—458.
- [5] Kolmogoroff A. N. and Dmitrieff N. A., *Vietviashtchiiesia slutchai-nyie processy*, Dokl. Akad. Nauk SSSR **56** (1) (1947), 7.
- [6] Lévy P., *Systèmes markoviens et stationnaires. Cas dénombrable*, Ann. Ec. Norm. Sup. **68** (1951), 327—381.

Connections between the Einstein-Infeld Approximation Method and the Perturbation Method

by

W. KRÓLIKOWSKI

Presented by W. RUBINOWICZ on June 8, 1954

The idea of the Einstein-Infeld approximation method was applied for the solving of the state equations of the quantum theory. It appears that in such a case this method is in a sense directly opposed to the Dirac, but equivalent to the stationary perturbation method.

Let us consider the state equation in the Schrödinger picture:

$$(1) \quad i\hbar \frac{\partial \Psi}{\partial t} = (\overset{0}{H} + \overset{1}{H}) \Psi,$$

assuming the operator $\overset{1}{H}$ to be a perturbation of the operator $\overset{0}{H}$. The operators $\overset{0}{H}$ and $\overset{1}{H}$ are not here dependent on time.

As is well known [1], the Dirac perturbation method consists of the following procedure: firstly, by means of the unitary transformation:

$$(2) \quad \begin{cases} 0_I = e^{\frac{i}{\hbar} \overset{0}{H} t} 0 e^{-\frac{i}{\hbar} \overset{0}{H} t}, \\ \Psi_I = e^{\frac{i}{\hbar} \overset{0}{H} t} \Psi, \end{cases}$$

we get a new picture (interaction picture), where the state equation has the form

$$(3) \quad i\hbar \frac{\partial \Psi_I}{\partial t} = H_I(t) \Psi_I.$$

Next, we seek a solution of equation (3) in the form of the series

$$(4) \quad \Psi_I = \sum_{l=0}^{\infty} \Psi_I^{(l)},$$

in which the magnitude orders are arranged in accordance with the rule

$$(5) \quad \begin{cases} i\hbar \frac{\partial \Psi_I^{(0)}}{\partial t} = 0, \\ i\hbar \frac{\partial \Psi_I^{(l+1)}}{\partial t} = \overset{1}{H}_I(t) \Psi_I^{(l)} \quad (l \geq 0). \end{cases}$$

Rule (5) is justified by the smallness of the matrix elements of the operator $\overset{1}{H}$ appearing on the right side of equation (3).

Instead of (2) let us perform the unitary transformation defined by the formulae:

$$(2') \quad \begin{cases} 0_B = e^{\frac{i}{\hbar} \overset{1}{H} t} 0 e^{-\frac{i}{\hbar} \overset{1}{H} t}, \\ \Psi_B = e^{\frac{i}{\hbar} \overset{1}{H} t} \Psi. \end{cases}$$

In the new picture the state equation assumes the form:

$$(3') \quad i\hbar \frac{\partial \Psi_B}{\partial t} = \overset{0}{H}_B(t) \Psi_B.$$

Let us introduce parameter E (of energy dimension) into equation (3'), using the substitution

$$(6) \quad \Psi_B = u_B(t) e^{-\frac{i}{\hbar} Et};$$

then we get

$$(3'') \quad i\hbar \frac{\partial u_B}{\partial t} = (\overset{0}{H}_B(t) - E) u_B.$$

Now, if we formally apply the idea of the Einstein-Infeld approximation method [2] to the state equation (3''), we shall find what condition the former imposes on the parameter E . Thus we shall try to find the solution of equation (3') by means of the series:

$$(4') \quad u_B = \sum_{l=0}^{\infty} u_B^{(l)},$$

in which the magnitude orders are arranged according to the rule

$$(5') \quad \begin{cases} 0 = (\overset{0}{H}_B(t) - E) u_B^{(0)}, \\ i\hbar \frac{\partial u_B^{(l)}}{\partial t} = (\overset{0}{H}_B(t) - E) u_B^{(l+1)} \quad (l \geq 0). \end{cases}$$

By means of the substitution

$$(7) \quad u_B^{(0)} = e^{\frac{i}{\hbar} \overset{1}{H} t} u^{(0)}$$

the first of the equations (5') is reduced to the eigenvalue problem for the operator $\overset{0}{H}$:

$$(8) \quad (\overset{0}{H} - E) u^{(0)} = 0.$$

This problem defines the eigenvalues E and eigenfunctions $u^{(0)}$ (the latter do not depend on time).

The equation (8) is the desired condition for the parameter E .

From the remaining equations (5'), if we perform simple calculations in which equations (7) and (2') are used, we get

$$(9) \quad u_B^{(l)} = e^{\frac{i}{\hbar} \overset{1}{H} t} \underbrace{(\overset{0}{E} - \overset{0}{H})^{-1} \overset{1}{H} (\overset{0}{E} - \overset{0}{H})^{-1} \overset{1}{H} \dots (\overset{0}{E} - \overset{0}{H})^{-1} \overset{1}{H}}_{l \text{ times}} u^{(0)},$$

where the operation $(\overset{0}{E} - \overset{0}{H})^{-1} \overset{1}{H}$ is repeated l times. We now see that rule (5') for the arrangement of the magnitude orders — derived from the idea of the Einstein-Infeld approximation method — is justified here by the smallness of the matrix elements of the operator $\overset{1}{H}$ in the exponent of the function $\exp(i \overset{1}{H} t / \hbar)$ on the left side of (3').

Finally, applying (2'), (6), (4') and (9), we get the following solution for the state equation (1):

$$(10) \quad \begin{aligned} \Psi &= \sum_{l=0}^{\infty} \underbrace{(\overset{0}{E} - \overset{0}{H})^{-1} \overset{1}{H} (\overset{0}{E} - \overset{0}{H})^{-1} \overset{1}{H} \dots (\overset{0}{E} - \overset{0}{H})^{-1} \overset{1}{H}}_{l \text{ times}} u^{(0)} e^{-\frac{i}{\hbar} E t} = \\ &= [1 + (\overset{0}{H} - E)^{-1} \overset{1}{H}]^{-1} u^{(0)} e^{-\frac{i}{\hbar} E t}. \end{aligned}$$

Taking a complete set α of commuting observables including the energy $\overset{0}{H}$, we get equation (10) in the following form:

$$\Psi = \sum_{l=0}^{\infty} \sum_{\alpha_1, \alpha_2, \dots, \alpha_l} |\alpha_1\rangle \frac{\langle \alpha_1 | \overset{1}{H} | \alpha_2 \rangle \langle \alpha_2 | \overset{1}{H} | \alpha_3 \rangle \dots \langle \alpha_l | \overset{1}{H} | u^{(0)} \rangle}{(E - E_{\alpha_1})(E - E_{\alpha_2}) \dots (E - E_{\alpha_l})} e^{-\frac{i}{\hbar} E t}.$$

The above formula represents the stationary perturbation solution of state equation (1).

Institute of Physics, Polish Academy of Sciences
Institute of Theoretical Physics, University of Warsaw

REFERENCES

- [1] Dirac P. A. M., *The Principles of Quantum Mechanics*, 3rd edition, Oxford 1947, p. 172.
- [2] Einstein A., Infeld L., Hoffmann B., *Ann. of Math.* **39** (1938), 66.

Absorption in Al of the Positron Radiation of ^{13}N

by

T. GRABOWSKI and L. NATANSON

Communicated by A. SOLTAN at the meeting of June 21, 1954

The decrease in the counting rate when a metal foil is placed between a source of β radiation and a G.M. counter is the cumulative effect of several physical processes. The most important of these is the ionization of the absorbing medium by the β electrons and their scattering. The β electrons lose energy upon ionization, and by scattering their effective path is lengthened. Some may emerge from the foil having suffered a deflection from their original direction so that they do not enter the counter window.

This is not a simple problem for rigorous theoretical treatment in view of the complication of the processes involved and of the fact that the original electron beam entering the foil has energies spread over a continuous spectrum. Such a treatment should be based on the well-known Bethe-Bloch formula [1], [2], [3] and on the theory of electron scattering as developed by Williams [4] and others.

The present note is an account of measurements of the absorption in Al of the β^+ radiation from ^{13}N . The shape of the spectrum of this radiation has been investigated by several authors [5], [6], [7]. It appears to be of the simple Fermi type. A search for γ radiation associated with the positron emission led to negative results.

A simple apparatus was used. The positron active ^{13}N was produced in the reaction $^{12}\text{C}(\alpha, n)^{13}\text{N}$. A graphite target was directly irradiated with deuterons accelerated in a high tension cascade tube to an energy of about 750 KeV. The irradiation lasted for 10 minutes, the deuteron current being maintained at 150 μA . In order to reduce back-scattering, thin sources were made consisting of fine tissue-paper stretched on a wooden frame and blackened with irradiated graphite in which ^{13}N was occluded. The active spot on the tissue-paper had usually a circular shape and a diameter of a few millimetres. The preparation of a source took no more than 5 minutes after the irradiation was ended. There was no apparent shortening of the half-life due to leakage of ^{13}N from the thin graphite layer. The in-

tensity of sources of this type was amply sufficient. Half an hour after irradiation the counter registered over 1000 pulses per minute when no absorbing foils were used except the Al foil, 0.04 mm. thick, of which the counter window was made.

The counter was enclosed in a metal box with an aperture of 17.6 mm. diameter in the top. A counter window of the same shape and a diameter about 15 mm. was placed axially under this aperture at a depth of 13 mm. The absorbing foils were laid on the box so as to cover the aperture. The source on its wooden frame was held at a distance of some 100 mm. above the counter window. The absorbing foils, measured with a precision screw micrometer, proved to be uniform in thickness within 2%. The average thickness was 0.259 mm.

The number of counts corrected for source decay and background was plotted against absorber thickness. In the interval above approximately 80 mg./cm.² and below 400 mg./cm.² it followed closely an exponential function of the form

$$N = N_0 \exp \mu d,$$

where μ is a constant coefficient and d the absorber thickness.

For the lowest value of absorber thickness absorption may have been somewhat anomalous, the necessary conditions not yet having been attained for the process to take the character of positron diffusion through the medium [8], [9]. On the other hand, above a certain thickness the number of counts remained practically constant when more foils were added. Presumably all β positrons were then absorbed and the counter registered only annihilation photons.

Thus the plot of the logarithm of the number of counts vs. absorber thickness has a rectilinear sloping-down section and horizontal section. The value of absorber thickness corresponding to the point of intersection between an extrapolation of the first of these with the second is by definition the "practical range" of the radiation (Fig. 1).

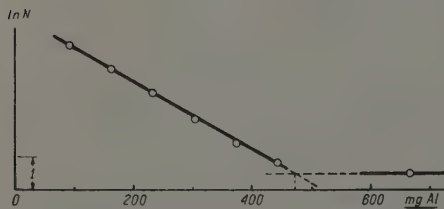


Fig. 1

The value of the absorption coefficient as computed from the results of our measurements is

$$\mu = 10.6 + 0.3 \text{ cm.}^2/\text{g.},$$

and the practical range (taking absorption in air into account)

$$R = 0.47 + 0.01 \text{ g./cm.}^2.$$

Using this value in the empirical Feather formula corrected by Widowsen and Champion [10], which gives the relation between the range in

Al and E_0 as the maximum energy of the spectrum, we obtain

$$E_0 = 1.185 \text{ KeV.}$$

This agrees within 1.5% with data from magnetic spectrometer studies

Institute of Physics, Polish Academy of Sciences

REFERENCES

- [1] Bethe H., *Zs. f. Phys.* **76** (1932), 293.
- [2] — *Ann. d. Phys.* **16** (1933), 285.
- [3] — *Zs. f. Phys.* **81** (1933), 363.
- [4] Williams E. J., *Phys. Rev.* **58** (1940), 292.
- [5] Cook C. S., Langer L. M., Price H. C. Jr. and Sampson M. B., *Phys. Rev.* **74** (1948), 502.
- [6] Siegbahn K. and Silatis K., *Ark. Math. Astr. och Fysik (A)* **32** (1945).
- [7] Hornyak W. F., Dougherty C. B. and Lauritsen T., *Phys. Rev.* **74** (1948), 1727.
- [8] Bothe W., *Zs. f. Phys.* **54** (1929), 161.
- [9] — *Hb. d. Phys.* **22/2** (1933), 23.
- [10] Widdowson E. E. and Champion F. C., *Proc. Phys. Soc.* **50** (1938), 185.

Photoconductive Lead Telluride Layers

by

H. CHECIŃSKA and L. SOSNOWSKI

Presented by A. SOŁTAN on June 21, 1954

Microcrystalline layers of lead telluride were obtained, showing, at liquid air temperature, high sensitivity to infra-red radiation.

Lead telluride was prepared by fusing pure elements *in vacuo*. Samples were used which contained either an excess of tellurium or of lead above the stoichiometric proportion. The best results were obtained with lead telluride containing a 3% excess of lead. This material was therefore subjected to further tests.

The layers were formed by a method of vacuum evaporation worked out by one of the authors [1], [2]; about 1 mg. of PbTe was used for each cell. The conductivity, photoconductivity and thermoelectric power were measured at the several stages of production of a sensitive layer. Over fifty experimental activations were performed; finally, 15 cells were produced with a sufficient degree of reproducibility.

Photosensitivity was observed only in the layers subjected to the influence of oxygen.

Layers formed *in vacuo* (pressure below 10^{-6} mm. Hg) showed conductivity of the *n*-type, as judged by observation of the thermal e. m. f. Conductivity was of the order of magnitude of $10 \Omega^{-1} \text{cm.}^{-1}$, being almost independent of temperature between 90°K and 300°K .

Under the influence of oxygen, conductivity changes from the *n* to *p* type; even the presence of oxygen at room temperature and a pressure of 10^{-3} mm. Hg were sufficient to cause such a change.

The conductivity of sensitive layers ranged from $0.1 \Omega^{-1} \text{cm.}^{-1}$ to $1 \Omega^{-1} \text{cm.}^{-1}$ at room temperature; at liquid air temperature the conductivity was more than 1000 times lower.

Spectral response was not investigated thoroughly; rough estimations indicate a limiting wavelength at about 4.75μ in agreement with data published by others [3], [4], [5]. Sensitivity at liquid air temperature is comparable with the best PbS cells; at room temperature only traces of sensitivity remain.

PbTe layers activated by our method remain sensitive when subjected to the influence of atmospheric air. Slight changes in properties took place shortly after the opening of the cells; afterwards "open" cells remained stable. The first "open" layers retained full sensitivity for more than one year.

This is a valuable property, which enables us to experiment freely on sensitive layers and which can be used conveniently for the detection of infra-red radiation. Layers are made in glass envelopes, which are non-transparent to radiation above a 3μ wavelength. This necessitates the use of special windows made of sapphire and other materials. Our cells do not require such windows because the front wall of the glass envelope may be removed after the production of the sensitive layer. Similar "open" PbS cells have been made in our laboratory by T. Piwowski [6].

Institute of Physics, Polish Academy of Sciences

REFERENCES

- [1] Starkiewicz J., Sosnowski L. and Simpson O., *Nature, London*, **158** (1946), 28.
- [2] — *Nature, London* **159** (1947), 818.
- [3] Moss T., *Nature, London* **161** (1949), 766.
- [4] Simpson O. and Sutherland, *Phil. Trans. of the Roy. Soc. of London, Series A* **243** (1951).
- [5] Gibson A. F., *Proc. Phys. Soc., London, Series B*, **65** (1952), 197.
- [6] Piwowski T., *Bull. Acad. Polon. Sci., Cl. III*, **1** (1953), 185.

Kinetics of Photoconductivity in Thallium Sulphide

by

J. W. OSTROWSKI and L. SOSNOWSKI

Communicated by A. SOŁTAN at the meeting of June 21, 1954

Our investigations were concerned with microcrystalline layers of thallium sulphide prepared by a method described by A. Wolska [1].

Experimental method

For measuring the sensitivity and relaxation time of photoconductivity, the impulse method was used. The layer under investigation was illuminated by short pulses of light. These pulses were in addition to a much stronger constant background illumination.

It was found that both the relaxation time and the sensitivity were strictly dependent on the intensity of the background illumination. Full radiation from an incandescent lamp was used as the background illumination. Its intensity could be changed, in the ratio 1 to 10 000, by variation of the distance between the lamp and the layer.

Relaxation time

Two methods were used for measuring the relaxation time τ . In both of these the layer was illuminated by light pulses from a neon lamp connected to a square wave generator. A signal from the layer, after proper amplification, was applied to the vertical plates of an oscilloscope. In the first method an exponential impulse was applied to the horizontal plates from an RC system connected to the same square-wave generator as was the neon lamp. In the case of an experimental decay of photoconductivity, provided the proper value of RC is chosen, a straight line should be observed on the screen of the oscilloscope [2]. The wide range of values observed for τ (from 100 μ s to 30 000 μ s) and the variation in the shape of decay with the change in background illumination caused considerable difficulty. Considerable deviation from an exponential decay was observed.

The second method consisted essentially in measuring the dependence of the amplitude of the signal on the ratio of the pulse duration to the interval

between two consecutive pulses. It was possible to adjust the generator in such a way that during the interval between pulses the signal decayed to one half of its maximum value. In this case the time of the interval was equal to the halftime of the decay τ .

The times of increase and decay (decrease) were approximately equal. With a very low level of background illumination the time of decay (decrease) was longer than the time of increase. This difference amounted to about 50%.

Photosensitivity

Dark conductivity and the dependence of conductivity on the intensity of the background illumination were measured for all the layers investigated. Sensitivity was defined as $S = \frac{1}{\sigma} \cdot \frac{d\sigma}{dI}$. Knowing function $\sigma(I)$, one can calculate $S(I)$. Sensitivity can be obtained also by measuring the signal from the layer directly on the screen of the oscilloscope, using the same source of light impulses as for the measurements of τ . For low intensity the signal is proportional to the intensity of the light pulse; one can then put $S = \Delta\sigma/\sigma\Delta I$. Both methods lead to identical values for S .

Results

The values of conductivity σ , sensitivity S and decay time τ of photoconductivity as functions of intensity of the background illumination are shown in Fig. 1. All curves are drawn in double logarithmic scale. From the results obtained, the dependence of both τ and S on σ can be calculated

$$(1) \quad \tau = a\sigma^{-2}$$

$$(2) \quad S = b\sigma^{-3}.$$

As can be seen from Fig. 2, formula (2) agrees with the experimental results with great accuracy. The same is true for all the layers investigated. The experimental points deviate noticeably from the straight line

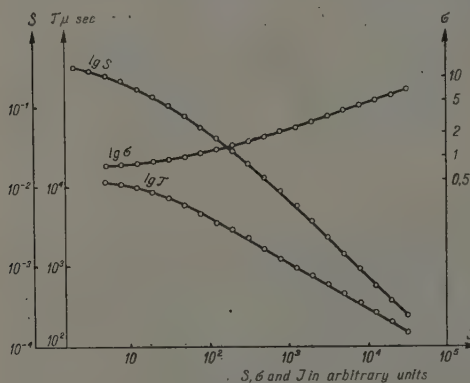


Fig. 1.

corresponding to formula (1), the mean inclination corresponds, however, to exponent 2 with considerable accuracy.

Interpretation of the results

The change in conductivity under the influence of radiation may be due either to a variation of the concentration of free carriers of current

(electrons and holes) or to a change in their effective mobility (barrier mechanism of the photoconductivity). Both causes may also be operative simultaneously. A. Wolska [1] has shown that in the Ti_2S layers investigated by her the majority of carriers are holes (conductivity of p -type). The straight line relations shown in Fig. 2 indicate that the same type of carrier is responsible for all dark current and photocurrent. The empirical relations found by us prove that in the material investigated the most important factor operating is the concentrative mechanism of photoconductivity, i. e. conductivity is proportional to the concentration of carriers

$$(3) \quad \sigma \sim n.$$

This may be seen from the behaviour of the ratio $S\sigma/\tau$ [3], which in our case can be easily found from equation (1) and (2)

$$(4) \quad S\sigma/\tau = \text{const.}$$

This ratio remains constant to within 30%, whereas S , σ and τ change in orders of magnitude. In each concentration theory $dn \sim \tau dI$, because increase of concentration is proportional both to number of carriers produced in unit time by radiation i. e. to dI and to the average life time of a carrier. But

$$S = \frac{1}{\sigma} \frac{d\sigma}{dI} = \frac{dn}{ndI} \sim \frac{\tau}{n},$$

$$\text{accordingly } \frac{S\sigma}{\tau} \sim \frac{S\sigma}{\tau} = \text{const.}$$

From equations (1) and (3) it can be seen that the probability of recombination W is proportional to the square of the concentration of free carriers

$$(5) \quad W = \frac{1}{\tau} = \alpha n^2.$$

Recombination is then a second order process, in which two holes (electrons) take part simultaneously. The energy of recombination cannot be given over to the lattice, part of it at least must be taken by another free carrier. In the theory of recombination direct interaction between electrons should be taken into account, apart from interaction between electrons and lattice vibrations (phonons). Our knowledge of recombination process is still very meagre. It is feasible to suppose that a similar relation may take place in other semiconductors. Recent results published by Moss [4] indicate that this is the case in PbS.

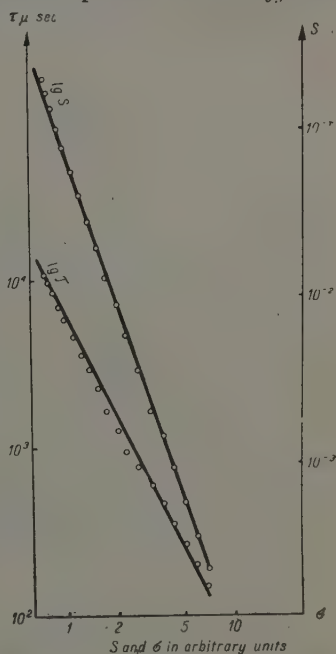


Fig. 2.

From (5) we get the following kinetic equation:

$$(6) \quad \frac{dn}{dt} = \gamma I + \alpha n_0^s - \alpha n^s.$$

The first term on the right hand side of the equation corresponds to the number of carriers produced in unit time by light, the second — to the n_0 of carriers produced by thermal vibration (n_0 — concentration of carriers in dark). The last one corresponds to the number of recombinations. In equilibrium

$$(7) \quad \frac{dn}{dt} = 0 \quad \text{hence} \quad n^s - n_0^s = \frac{\gamma}{\alpha} I \quad \text{and} \quad \sigma^s - \sigma_0^s = cI.$$

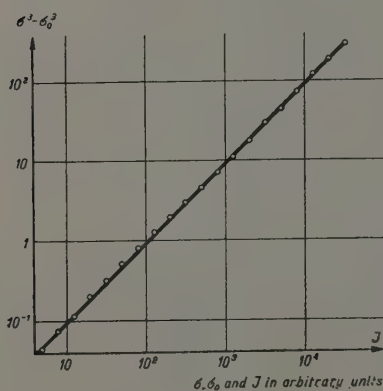


Fig. 3.

Experimental values of $\sigma^s - \sigma_0^s$ in function of I are shown in double logarithmic scale in Fig. 3; agreement with formula (7) is perfect. The solution of equation (6) in the non-stationary case gives the shape of a decay curve. The shape is in general a complicated one; it becomes almost exponential in the case of a strong background illumination I and small pulses. A. Wolska [1] has discussed many observed properties of Ti_2S photoconductive layers on the basis of the barrier theory. The internal photovoltaic effect was regarded especially as a proof of the existence of barriers. The occurrence

of barrier effects in Ti_2S layers seems to be proved beyond doubt. Our results show, however, that barriers are not the dominating factor determining conductivity. An exact comparison of the relaxation of photoconductive and photovoltaic effect in these layers should help us to understand better the rôle of barriers.

Further experiments in connection with this are being carried out.

Institute of Physics, Polish Academy of Sciences

REFERENCES

- [1] Wolska A., Bull. Acad. Polon. Sci., Cl. III, **1** (1953), 179.
- [2] Chmielewski M. and Sosnowski L., Bull. Acad. Polon. Sci., Cl. III, **1** (1953), 119.
- [3] Gibson A. F., Proc. Phys. Soc. B, **64** (1951), 603.
- [4] Moss T. S., Proc. Phys. Soc. B, **66** (1953), 993.

Microstructure of Photoconductive Lead Sulphide Layers

by

A. FELTYNOWSKI, I. GLASS, T. PIWKOWSKI, A. TORUŃ

Presented by A. SOŁTAN on June 22, 1954

The purpose of this study was to examine the microcrystalline structure of photoconductive PbS layers, including the shape and size of the separate crystals, and, by means of electron diffraction, the chemical constitution of the layers.

As far as we could ascertain, no electron microscope investigations appear to have been made of photoconductive PbS layers, probably because of technical difficulties in the preparation of the specimens. We have overcome this difficulty by an examination of extremely thin layers which were still photoconductive.

Our investigations were confined to the so-called "open" PbS layers, i. e. layers which retain the property of photoconductivity when exposed to the atmosphere. On the basis of earlier studies by Sosnowski and others [1], one of us (T. P.) has developed a method for processing such "open" layers [2].

The PbS layer to be examined by the electron microscope was deposited by evaporation on a polished glass surface, such as is ordinarily used as the substrate material in photocells. The central area of the glass plate was coated more thickly than the periphery. The evaporated layer was removed from the glass surface by means of a thin (c. 100 Å) formvar film. The PbS layer, if sufficiently thin, was completely removed in this way.

It was found that in the region of the periphery, where the layer is thin, it is not uniform even in areas at a constant radial distance from the condensation centre. This is due to the manner of condensation of thin films [3].

In addition to coherent regions, opaque to the electron beam, the electron micrographs also show regions embracing apparent crystals (Fig. 1). These are oblong in shape, 250—1000 Å wide and 900—3000 Å long; they are not randomly distributed, but show a tendency to form clusters. Farther from the centre can be seen isolated single crystals (Fig. 2). Attention

is drawn to the fact that the crystal edges are not sharp; this is not due to defects in focussing.

The photoconductivity of the layer under investigation was verified.

The same layer was then investigated by means of electron diffraction [4]. Figure 3 represents the diffraction pattern of this layer, using 71.5 kV

TABLE

No.	D mm.	Intensity	Plane indices $h\ k\ l$	$A = \frac{D}{\sqrt{h^2 + k^2 + l^2}}$
1	2	3	4	5
1	8.50	very strong	1 1 1	4.91
2	9.23	very strong	2 0 0	4.62
3	9.83	faint	(2 0 0)	(4.92)
4	10.67	faint		
5	11.21	faint		
6	12.25	faint		
7	13.39	faint	(2 2 0)	(4.74)
8	14.40	very strong	2 2 0	5.10
9	14.89	very faint		
10	16.37	strong	3 1 1	4.94
11	16.88	very faint		
12	17.20	medium	2 2 2	4.97
13	17.94	very faint		
14	18.63	faint	4 0 0	4.66
15	19.55	very faint	(4 0 0)	(4.89)
16	19.97	very faint		
17	21.38	strong	3 3 1	4.90
18	21.76	medium	4 2 0	4.87
19	22.06	very faint		
20	22.72	faint		
21	23.34	very faint		
22	23.98	medium	4 2 2	4.90
23	24.48	faint		
24	25.15	rather marked	$\begin{Bmatrix} 3\ 3\ 3 \\ 5\ 1\ 1 \end{Bmatrix}$	4.84
25	25.40	faint		
26	25.94	very faint		
27	26.58	faint		
28	27.52	medium	4 4 0	4.86
29	28.36	very faint		
30	29.08	faint	5 3 1	4.92
31	29.60	faint	$\begin{Bmatrix} 6\ 0\ 0 \\ 2\ 4\ 4 \end{Bmatrix}$	4.93
32	32.90	medium	6 2 2	4.96
33	33.70	medium	4 4 4	4.86

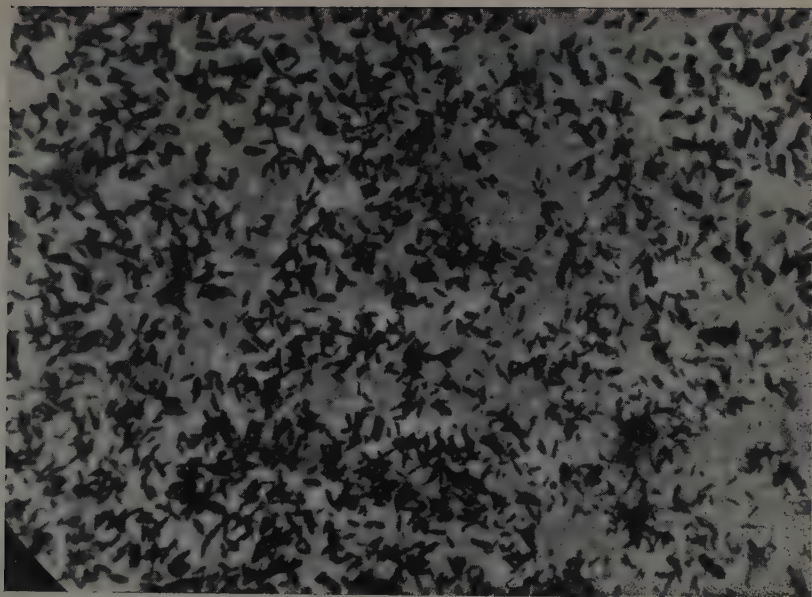


Fig. 1. Electron micrograph of the peripheral region of a PbS layer. Apparent crystals are evident. Magnification 12,000 x



Fig. 2. Electron micrograph of a PbS layer at a distance farther removed from condensation centre than shown in Fig. 1. Isolated single crystals are evident. Magnification 12,000 x

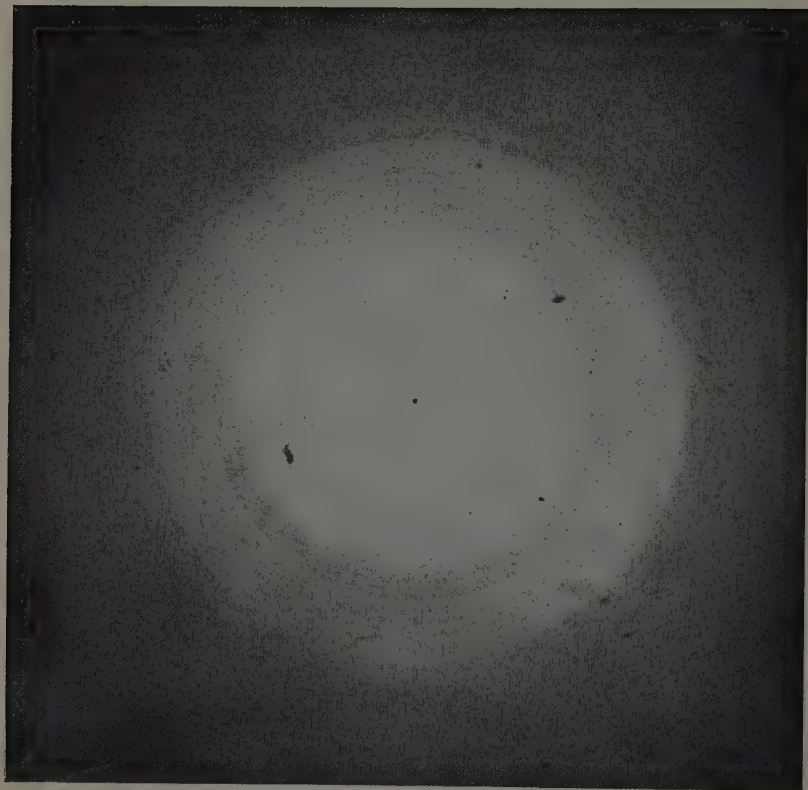


Fig. 3. Diffraction pattern of PbS layer

electrons. The diffraction pattern shows that in the area of electron transmission there was a sufficient quantity of crystals to give a representative pattern.

The table gives ring diameters. In column 4, for rings of stronger intensity, plane indices are given on the assumption of a face-centred cubic structure. Column 5 gives the values

$$A = \frac{D}{\sqrt{h^2 + k^2 + l^2}}$$

which should be constant to an accuracy of 0.7% [5].

There is a considerable deviation from the mean value of A in the case of the strong rings Nos. 2 and 8 and the faint ring No. 14. In addition to these rings, there were considerably fainter ones (Nos. 3, 7, 15), for which the value A shows a much smaller deviation from the mean. The same deviations were to be found both for different electron energies (40, 50, 55, 65 kV) and for PbS layers from different cells, deposited on glass as well as on mica.

The diffraction pattern (Fig. 3) shows also the presence of many rings of faint intensity which cannot be ascribed to PbS.

These facts can be related to the presence in the photoconductive layer of crystals other than PbS as well as to lattice deformation. Both may be connected with the method of processing of "open" layers.

The determination of the structural constitution on the basis of diffraction patterns is the subject of further investigations.

The authors are grateful to Professor L. Sosnowski for suggesting this investigation and for his constant advice.

Institute of Physics, Polish Academy of Sciences

REFERENCES

- [1] Sosnowski L., Starkiewicz J., Simpson O., *Nature* **159** (1947), 818.
- [2] Piwkowski T., *Bull. Acad. Polon. Sci., Cl. III*, **1** (1953), 185.
- [3] Blois M. S., Rieser L. M., *J. Appl. Phys.* **25** (1954), 338.
- [4] Wilman H., *Proc. Phys. Soc.* **60** (1948), 117.
- [5] Laue M. v., *Materiewellen und ihre Interferenzen*, Leipzig 1948.

On the Structure of Some Aliphatic Nitro-Compounds

by

T. URBĄŃSKI

Communicated at the meeting of May, 17, 1954

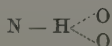
It has been shown previously [1], that some aliphatic nitro-compounds do not show a clear absorption maximum in ultra-violet light near to $\lambda = 270 \text{ m}\mu$, which is characteristic for a nitro-group.

It has been suggested that this may be due to the formation of hydrogen bonds, which would form six-member rings, composed of the nitro-group and hydroxyl- or amino-group.

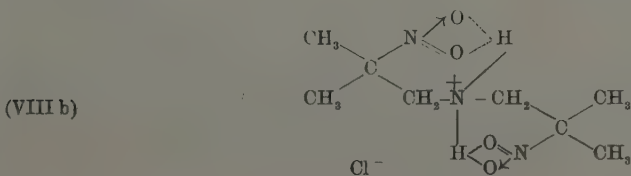
However, it was unexplained why, in order to suppress the absorption maximum of a nitro-group, two hydroxyl-hydrogen atoms and only one hydrogen atom of an amino-group are necessary. It was suggested that this might be due to the strong electron-repelling property of the amino-group combined with the electron-attracting property of the nitro-group.

This would be in accordance with the present interpretation of the nature of hydrogen bonds which can be regarded as partly electrostatic [2].

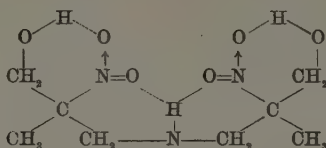
Independently of this explanation, it seems possible also to give another interpretation, based on the results of the structural X-ray analysis of aminoacids, particularly of glycine [3]. These experiments lead to the conclusion that a hydrogen atom belonging to an amino-group can be bound with two oxygen-atoms by means of two hydrogen bonds, i. e.



Thus, the structure of the hydrochloride of (VIII) and of the free base (X), which do not show a maximum in ultra-violet light, could be written as shown below — (VIII b) and (X a):



(Xa)



It can be shown, with the help of atomic models, that in the structure (VIIIb) the length of the hydrogen bonds is smaller than 2 \AA and that in the structure (Xa) it is smaller than 1.5 \AA .

In this case it would not be necessary to suppose two limiting structures, as shown in the preceding paper [1], for compound (X).

Institute of Organic Synthesis, Polish Academy of Sciences

REFERENCES

- [1] Urbański T., Bull. Acad. Polon. Sci. CL III, **1** (1953), 239.
- [2] Chichibabin A. E., Sierghieyeff P. G., *Osnovnyie nachata organicheskoy khimii*, Moscow—Leningrad 1953, 113.
- [3] Kitaygorodski A. I., Acta Phys. Chim. USSR., **5** (1936), 749; Albrecht G., Corey R., J. Am. Chem. Soc. **61** (1939), 1087; Shugam E. A., Uspiehi Khimii **19** (1950), 157.

Über die Trennung und Aufarbeitung des Picolinteerbasengemisches

von

J. BARTZ

Eingereicht von J. SUSZKO am 10 April 1954

In letzter Zeit widmete man viel Aufmerksamkeit dem Problem der Trennung der Picolinteerbasen. Eine einwandfreie Trennungsmethode ist anscheinend bis jetzt nicht allgemein bekannt.

Die Siedepunkte der beinahe untrennbar destillierenden Basen befinden sich im Temperaturbereiche von 140° C. bis 145° C. Im engeren Siedebereiche 142-145° C. findet man ungefähr gleiche Teile von 3-Picolin, 4-Picolin und 2,6-Lutidin. Aus diesem Gemisch scheint es vorteilhaft zu sein, die Komponenten nacheinander zu entfernen, wobei man mit 2,6-Lutidin beginnt. In der Praxis bedient man sich zu diesem Zwecke der Zinksalze [1], der Chlorhydrate [2] oder man bindet die Basen mit Harnstoff zu einem Additionsprodukt.

In der zu besprechenden Methode wird anfangs das Gemisch der 3- und 4-Picolinen einer chemischen Trennung unterworfen und nachher auch die dreigrädige Picolinfraktion 142-145° C. aufgearbeitet.

Es wurde der Unterschied in der Reaktionsfähigkeit der Methylgruppen in der Stellung 2- und 4- gegenüber Methylgruppen in der 3- Stellung ausgenützt. Die Fähigkeit der Picoline mit Formaldehyd zu reagieren ist von der Lage der Methylgruppen abhängig. In Betracht kommen nur Methylgruppen, welche an die Kohlenstoffatome 2 oder 4 des Pyridinringes gebunden sind. Die Kohlenstoff-Stickstoffdoppelbindung gibt nämlich einem solchen 2-Methylpyridin gewisse Ähnlichkeit zum α -Methylketon, welches bekanntlich leicht in Aldolkondensationen eingehen kann. Diese Fähigkeit wurde für die Methylgruppe in der 3-Stellung nicht beobachtet.

Die Aldolreaktionen der 2- und 4-Picoline und des 2,6-Lutidins sind bereits bekannt. Es war jedoch fraglich, in welchem Ausmasse sie zur quantitativen Trennung der Basen ausgenützt werden können.

In älterer [3] und neuerer [4] Literatur findet man darüber nur unvollkommene Hinweise. Man hätte laut diesen Angaben ungefähr 40-prozentige Kondensation als maximale Ausbeute zu erwarten.

Zur Durchführung der Trennung der Methylbasen wurden verwendet:

I. Ein Gemisch der 3- und 4-Picoline.

II. Die dreigrädige Picolinfraktion 142-145° C.

Die ersten Versuche der quantitativen Ausscheidung des 4-Picolins aus dem 3- und 4-Methylpyridingemisch haben erwiesen, dass die Abscheidung mit Ausbeuten von 95% möglich ist. Von diesen Beobachtungen ausgehend, wurden die drei nachstehenden Trennungsmethoden ausgearbeitet.

Ia. Die Kondensation wurde mit starkem Formalin durchgeführt. Die Menge des Formaldehyds war etwas höher als die stöchiometrisch berechnete. Versuche wurden auch mit kleinem Zusatz einer katalytisch wirkenden Substanz ausgeführt. Nachdem man die Kondensation durch Erwärmen unter Rückfluss beendet hatte, wurde das 3-Picolin mit Wasserdämpfen abgetrieben und im Destillat mit Benzol ausgezogen.

Ib. Werden die Reaktionsbedingungen des 3- und 4-Piculingemisches mit Formaldehyd etwas abgeändert, so erübrigt sich die Wasserdampfdestillation und an deren Stelle wird die Trennung mit Trichloräthylen oder Benzol ausgeführt. Benzol bildet mit 3-Picolin eine Lösung, wogegen 4-Methylpicolin sich als zweite Phase abtrennt.

Verfährt man nach einer der beiden oben angegebenen Vorschriften, so gewinnt man das 3-Picolin von einer handelsüblichen Reinheit von 95% in nahezu quantitativer Ausbeute, dagegen das 4-Picolin wird im Betrag von 97% gebunden.

Ic. Das Gemisch der 3- und 4-Picoline wurde mit einer stöchiometrisch unzureichenden Menge Formaldehyd kondensiert. Durch Wasserdampfdestillation wurde das ganze 3-Picolin und der Anteil von 4-Picolin, welcher nicht gebunden wurde, übergetrieben. Zum Destillat wurde eine wässrige Suspension von Kupferchlorür [5] hinzugefügt, wobei der überwiegende Teil des 3-Picolins als Molekülverbindung gefällt wird. Nach Abscheiden des Niederschlages verbleiben im Filtrat die 3- und 4-Picoline wiederum im ursprünglichen Verhältnis 1:1. Das Basengemisch wird aus der wässrigen Lösung mit Benzol ausgezogen und dient als Zusatz zur neuen Charge der 3- und 4-Picolinfraktion zwecks normaler Verarbeitung (wandert in den Prozess zurück).

Die Komplexverbindung des 3-Picolins mit Kupfer zersetzt man mit Natronlauge und treibt die Base mit Wasserdampf über. Das im Kolben übrigbleibende Kupferoxydul wird auf der Nutsche ausgewaschen. Wird nun das Kupferoxydul mit konzentrierter Salzsäure behandelt, so liefert es das nötige Reagenz in Form einer Suspension zur neuen Fällung des 3-Picolins. Bei Wiedergewinnung des Fällungsmittels sind die Verluste an Metall gering.

Die Oxydation des 4-Trimethylpicolins wurde mit Salpetersäure ausgeführt. Die Ausbeute belief sich auf 95%. Das salpetersaure Salz der Isonicotinsäure wurde nach einmaliger Kristallisation unmittelbar in üblicher

Weise esterifiziert, wobei durchschnittlich 70% Ausbeute, meist aber höhere, erreicht wurden.

II. Die Trennung der dreigrädigen Picolinfraction liess sich grundsätzlich auf dasselbe Prinzip zurückführen. Es wurde zunächst 4-Picolin in üblicher Weise abgeschieden und dann erst das 2,6-Lutidin in entsprechender Weise mit Formalin kondensiert. Aus dem zurückbleibenden, nicht gebundenen, Basengemisch kann 3-Picolin in üblicher Weise (Reinheit je nach Bedarf) gewonnen werden. Ungefähr 15% der Basen entging der Bindung und wird dem Anfangsreaktionsstadium wieder eingegliedert.

Nach allen oben skizzierten Methoden ist Formaldehyd zur Trennung unbedingt notwendig. Trotzdem erscheinen die Verfahren durchaus preiswert, da die Isonicotinsäure in Ausbeuten von 90% erhalten werden kann, anderseits das 3-Picolin je nach Bedarf in zwei Reinheitsgraden von etwa 99% oder 95% gewonnen wird.

Lehrstuhl für Organische Chemie an der Universität Poznań

SCHRIFTTUM

- [1] Rubzow M. W., Dokl. Akad. Nauk SSSR **89** (1953), 81.
- [2] Świątosławski W., Przem. Chem. **29** (1950), 591.
- [3] Königs W., Ber. **36** (1903), 2904.
- [4] Graf R., J. Prakt. Chem. **146** (1936), 88.
- [5] Öster. Pat. 172652, CA **47** (1953), 11259.

On the Tuffite Layer of the Upper Krosno Beds in the Dukla Region of the Carpathians

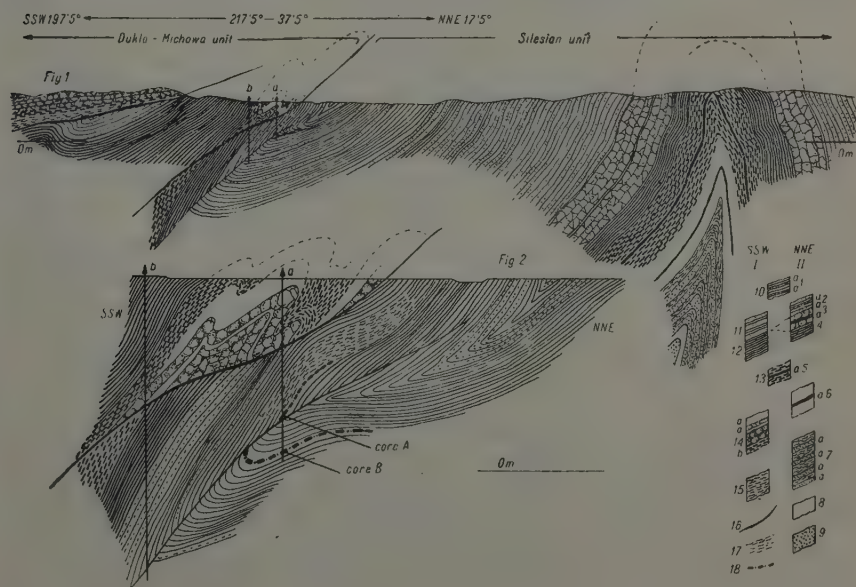
by

A. TOKARSKI and J. TOKARSKI

Presented by J. TOKARSKI on April 30, 1954

In the course of investigations of the deep geological structure of the Carpathians, the frontal zone of the Dukla-Michowa unit was examined by means of geological borings, the findings being later interpreted. The unit in question is thrust, in a northwardly direction, over the southern part of the Silesian unit [1], [2].

The section described could also have been extended northwards as far as the intersection with the extreme southern fold of the Silesian unit (Fig. 1).



Figs. 1 and 2.

Here, geological borings have shown the overthrust towards the north of the separated, secondarily folded, progressively overturned centre of the frontal structure of the Dukla-Michowa unit onto the undercutting, gently sloping dislocation. Here, the discordantly overturned wing of the northwardly overtoppled syncline, filled in its centre with Upper Krosno beds (Fig. 2), is covered by Cergowa sandstone and surrounded by squared out Cergowa and Menilite shales. The axial section of the plane of this syncline is well marked by the root observed on the surface, the change of slopes in the centres of the borings, as well as by the normal position of hieroglyphs in the lower part of the profile. In boring "a", in the Upper Krosno schists, the geologist J. Kruczek found, above and below the axial plane, at depths of

$$A = 246.60 \text{ to } 249.80 \text{ metres and}$$

$$B = 306.40 \text{ to } 308.60 \text{ metres,}$$

a rock which proved to be tuffite*).

Owing to the importance of the discovery of an element of this kind in the profile of the Krosno beds, the tuffite was petrographically analysed in great detail, and the following results were arrived at:

By its megascopic appearance the tuffite nucleus is only very slightly different from the contiguous massive argillaceous shales. It is remarkable by its grey colour and its thoroughly homogeneous pelitic structure. It absorbs water avidly and specimens, immersed in water, decompose into two fractions, one of which sinks rapidly to the bottom, while the other, distinctly colloidal, forms a durable suspension. The rock, particularly when examined in sections prepared for the microscope, has a unique appearance, which is brought out under polarised light. Above all, we met with minute fresh fragments of phenocrysts of quartz, feldspar, biotite, and sporadic heavy minerals. The latter stood out in relief above the surrounding material. These phenocrysts, especially those of quartz and feldspar, are irregularly fractured, giving a picture of a typical pyroclastic rock. The olive-green biotite is generally hexagonally shaped. Here and there are also secondary admixtures of carbonate rhombohedra (dolomite?). The rock background seen in ordinary daylight is faintly differentiated. Under polarised light its very advanced process of hydrolysis is clearly visible, due to the accumulation of feldspar and volcanic glass decomposition products.

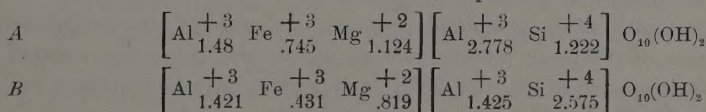
The generally known pictures of classical bentonites do not differ from those given by the thin sections of this rock. As to the variety of the tuffite, this could be ascertained through rational and precise chemical analysis. Such an analysis was made on two samples drawn from the upper and lower parts of the boring, and its results are represented in the table.

*) In spot A there was obtained a 30 cm. core of actual tuffite rock (70° incline). In spot B there was obtained a 130 cm. core including 115 cm. of tuffite rock in its top part (30° incline).

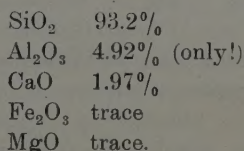
TABLE
Rational analysis of Lipowica tuffite

Per cent of weight	Soluble in HCl		Not soluble in HCl		Molar percentage soluble in HCl		Normal analy- sis. Per cent of weight
	A	B	A	B	A	B	A
SiO ₂	4.40	12.80	56.82		22.04	46.62	61.62
TiO ₂	0.10	0.12	—		—	—	0.10
P ₂ O ₅	none	none	—		—	—	—
Al ₂ O ₃	12.59	12.05	3.00		37.13	25.86	15.66
Fe ₂ O ₃	3.53	2.82	trace	53.81	6.64	3.87	3.53
MnO	none	none	—		—	—	—
CaO	1.50	0.89	1.12		8.02	3.48	2.62
MgO	2.77	2.78	trace		20.67	15.02	2.77
K ₂ O	1.25	1.77	—		4.00	4.12	1.25
Na ₂ O	1.31	0.29	—		1.50	1.03	0.31
+ H ₂ O	—	—	3.99	4.31	—	—	3.99
— H ₂ O	—	—	8.15	7.58	—	—	8.15
Σ	26.45	33.52	73.08	65.70	100.00	100.00	100.09

Structural formulas for the parts soluble in HCl



The part which was soluble in HCl consisted of bentonitic material and the rest (of which there was the greater part) was recognized as volcanic glass. In spite of advanced devitrification, this glass showed clear traces of its original structure — mainly “pumice” and “globular”. It was very acid, with a much lower light refraction coefficient than Canada balsam. Its analysis, carried out separately, showed, besides H₂O, the presence of



From these data the authors deduced that the tuffite had been decomposed hydrolytically and transformed to the extent of about 50%, into a secondary product, namely bentonite (the part soluble in HCl, taking into account H₂O).

The application of the modern method of representation of chemical structures of this kind, propounded by C. S. Ross and S. B. Hendricks [3],

gave pictures of bentonitic structure in the case of both the examined samples, which are presented in the table.

It would appear, therefore, that Carpathian bentonites from the Krosno beds markedly diverge in structure from all those encountered so far, in that the silicon kations in tetrahedral co-ordinations are replaced to a much larger extent by aluminium kations. This is, therefore, an as yet undetermined new link of the isomorphic montmorillonite series.

Had the rock been examined by X-rays, it might perhaps have been shown that the excess of alumina was concentrated in the form of hydrates. Future investigations may confirm this hypothesis; Polish tuffites would then have to be classed with laterites and would constitute an important piece of paleogeographic evidence.

The normal analysis of the tuffite gave the index numbers listed in the table. These figures differ from the Tortonian tuffites previously found in the Carpathian forehills, principally by being representative of any magma of a more basic type. Potassium greatly predominates, in the discovered rock, over sodium. Hence the difficulty in classifying it exactly in the magmatic series. These tuffites generally appear to have their origin from dacitic magma, which has undergone secondary hydrolysis. Hydrolysis produces, above all, a drop in the sodium content, hence among alkalis, a relatively considerable accumulation of potassium, adsorbed during diagenesis by the formation of colloidal bentonite.

The appurtenance of the examined products to dacites is also confirmed by the analysis of feldspar phenocrysts in which the percentile content of anorthite varies between 22 and 55%, and higher. Alkali feldspars appear very sporadically in this group of components.

Transparent heavy minerals were extracted from the 10-gram samples in very small quantity (there being barely enough for a simple microscopic slide). Here is the list of these minerals: (in percent)

Garnet	14%	Rutile	1%
Zircon	7%	Brookite	1%
Tourmaline	1.5%	Hornblende	5%
Staurolite	1%	Biotite	54%
Apatite	17%	Chlorite	3%

and a trace of Corundum.

The slide showed, moreover, a relation of opaque to transparent minerals of 28:72.

This list resembles data which were previously collected for Tortonian tuffs in the Carpathian forehills [4]. It is worthy of note that biotite, which appears sometimes in large quantities in many of the concentrations of heavy minerals of the Krosno layers, is physiographically clearly different from that found in tuffites. The difference is one of shape and above all of colours: Krosno biotite, by its rubiginous colour, reminds one of the "exotic" biotites in the Bugaj granites.

The largest diameters of the major component of this rock (volcanic glass) range between 9μ and 135μ . The average diameter is 45μ .

The dispersion curve of the grain shows great similarity with the average tuffite glass curve examined in the centres of borings obtained in the Tortonian formation of the Carpathian forehills at Chodowice [5]. This proves that in each case the distance of the volcanic eruption centre was nearly the same (about 250 km.). It is also significant that in the Upper Krosno tuffites we found only traces of heterogeneous bodies, such as terrigenous elements of the sedimentary basin. Their considerable thickness, notwithstanding the considerable distance from the eruption centre, also proves the great force of volcanic action during that period in the Carpathian hinterland.

The recognition of the tuffite horizon in the part of the Carpathians under consideration has, for the sake of more extensive palaeographic, stratigraphic and tectonic formulations, a threefold significance, namely:

1. The tuffites which were discovered in the normal wing of the syncline, appear in the well-defined, typical stratigraphical profile of the southern part of the Silesian unit in the region of Jasło. Here, they are found above the Menilite shales in the following sequence:

- (i) transitory beds,
- (ii) black limy schists with "Krosno" type sandstone,
- (iii) Lower Krosno beds of the brittle thick-banked sandstone type,
- (iv) Middle Krosno beds in the form of plated, crusted sandstone with enclosure of grey shales,
- (v) Upper Krosno beds: grey shales with only occasional sandstone enclosures.

The tuffites appear in the Upper Krosno beds in this series, 2500 m. above the level top of Menilite shales. Therefore, the palaeographic phenomenon of volcanic dust sedimentation is, from the stratigraphical viewpoint, clearly localised in this spot.

Thus, a direction has been given to further search for tuffites and their derivatives, for correlation purposes.

The petrographic character of the tuffite here described, which is unlike that of the Tortonian tuffites found in the Carpathian forehills, fixes the uppermost limit for the possibility of acceptance (according to certain suggestions) of the Upper Krosno beds in the Miocene Period. Such an acceptance might, for example, be effected on the basis of general conceptions [6] and microfauna [7].

2. The tuffite horizon, found in both wings of the syncline, makes it imperative to connect the different faces of Krosno beds (the Silesian facies in the normal wing with the Dukla-Michowa facies in the overturned wing) by a continuous passage. These facies — apart from the greater thickness of the transitory layers of the southern face — differ principally by a lack of thick banks, a deficiency of brittle sandstone in the Lower Krosno layers

and by the stepping down of the crust facies to the transitory layer top. A similar conjunction of both the facies through the synclinal root has already been encountered in other sections of this syncline, both on the surface [8] and in borings. According to regional observations one may regard these sudden facial passages within the limits of the syncline as the final effect of gradual changes noted in successive profiles south of the Jasło parallel. For it is in this direction that there is a gradual reduction in the thickness of the thick-banked series of the Lower Krosno layers in favour of the growing thickness of the crust face of the Middle Krosno layers and of the transitory layer face. The disappearance of the thick-banked Lower Krosno sandstones above the Menilite shales appears to be balanced in the south by the appearance of similar sandstone, in this case Cergowa sandstone, under the shales.

3. The tuffite root between the two wings of the syncline indicates that the main course of the Dukla-Michowa overthrust runs within the limits of the layers of the series of same name. Instead of there being one sharp overthrust, it divides into three elements, which become more evident in their course from south to north (see Fig. 1 and 2). The three elements in question are:

- a) a small overthrust along the "tuffite" syncline axis;
- b) a tectonic reduction and crumpling of its overturned flank;
- c) an overthrust of stiff masses of Cergowa sandstone.

Soil Science Institute, Cracow

REFERENCES

- [1] Teisseyre H., *Sprawozdanie z badań geologicznych w 1929 r. w okolicy Dukli*, Spraw. P. I. G., vol. V, Warsaw 1930.
- [2] — *Zarys budowy geologicznej Karpat dukielskich*, Spraw. P. I. G., vol. VII, Warsaw 1932.
- [3] Ross C. S. and Hendricks S. B., *Minerals of the Montmorillonite Group*, Washington 1945.
- [4] Parachoniak W., *Tortońska facja tufitowa między Bochnią a Tarnowem*, Acta Geol. Pol. 4 (1954).
- [5] Tokarski J., *Z petrografii utworów tufogenicznych podkarpackiej formacji solonośnej*, Bull. Intern. Acad. Pol., No. 1—3 A (1939).
- [6] Opolski Z., *O stratygrafii warstw krośnieńskich*, Spraw. P. I. G. vol. VII, Warsaw 1933.
- [7] Huss F., *Mikrofauna warstw krośnieńskich*, manuscript, 1952.
- [8] Tokarski A., *Zachodnia część fałdu Mrukowej, Nafta* (1946).